INITIAL STREAK CAMERA MEASUREMENTS OF THE S-BAND LINAC BEAM FOR THE UNIVERSITY OF HAWAI`I FEL OSCILLATOR*

A.H. Lumpkin, Fermi National Accelerator Laboratory, Batavia, IL 60510 USA
M.R. Hadmack, J.M.D. Kowalcyzk, E.B. Szarmes, and J.M.J. Madey
University of Hawai`i at Mānoa, Department of Physics and Astronomy, Honolulu, HI,USA

Abstract

Experiments with a Hamamatsu C5680 dual-sweep streak camera have been performed on the Mark V Free-electron Laser (FEL) oscillator linac beams at the University of Hawai`i. The bunch length and phase of the e-beam were evaluated throughout the macropulse duration via both optical transition radiation and coherent spontaneous harmonic radiation sources. Bunch lengths of 3-5 ps FWHM and phase slews of 7 ps over 2 μs are reported under lasing conditions.

INTRODUCTION

The S-band linac driven Mark V Free-electron Laser Oscillator (FELO) at the University of Hawai`i operates in the mid-IR at electron beam energies of 40-45 MeV with a four microsecond macropulse length [1]. Recently investigations of the electron beam micropulse bunch length and phase as a function of macropulse time became of interest for potentially optimizing the FELO performance. These studies involved the utilization of a Hamamatsu C5680 streak camera with dual sweep capabilities, depending on the vertical sweep and horizontal sweep units installed, and the transport of optical transition radiation (OTR) generated at an upstream Cu mirror, and of coherent spontaneous harmonic radiation (CSHR) [2] generated in the undulator to the streak camera location outside of the linac tunnel. Both a fast single sweep vertical unit and a synchroscan unit tuned to 119.0 MHz were used. Initial results include measurements of the individual CSHR (on the FEL7th harmonic at 652 nm) micropulse bunch lengths, the CSHR signal intensity variation along macropulse time, and a detected phase slew of 7 ps over the last 2.4 μs of the macropulse. Complementary OTR measurements were also evaluated and will be presented.

FACILITY ASPECTS

The UH Mark V linac with thermionic microwave rf gun, one S-band normal conducting accelerator, and beamline is schematically shown in Fig. 1. The S-band accelerating section provided 40- to 45-MeV beams before the diagnostics chicane. Micropulse charges of 40 pC were used typically with an rf macropulse duration of ~4 us. The macropulse repetition rate was 5 Hz.

The experimental conditions provided several challenges between the broadband OTR source which is quite weak with only 46 pC in a single micropulse, but quite strong if integrated over 4 μs (but heats up the screen) and the CSHR which was 1000 times stronger and narrowband at a harmonic of the 4.5-μm FEL fundamental. The 119.0 MHz synchroscan unit was phase-locked to the 24th subharmonic of the micropulse repetition rate. The OTR and CSHR pulse length and phase were measured with the Hamamatsu UV-visible C5680 streak camera system. The camera was a demo from Hamamatsu, and the synchroscan unit was on loan from Argonne National Laboratory. The synchroscan streak camera allowed tracking of the relative phase within the macropulse of sets of micropulses to about 200 fs. The OTR and CSHR were transported 7 m using mirrors and lenses to an optical enclosure (including a photodiode and the streak camera) located outside of the accelerator tunnel.

Table 1: Summary of Electron Beam Properties During Run

Parameter	Units	Values
Bunch charge	pC	46
Energy	MeV	40-45
Bunch length, (FWHM)	ps	2-5
Macropulse Length	μs	4

lumpkin@fnal.gov
'Work supported under Contract No. DE-AC02-07CH11359 with the United States Department of Energy and work at UH supported by United States Department of Homeland Security grant number 20120-DN-077-AR1045-02.

ISBN 978-3-95450-126-7

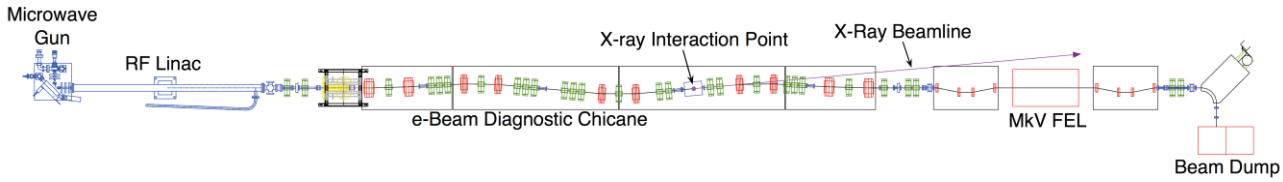

Figure 1: Schematic of the Mark V FEL beamline with microwave rf gun, S-band linac, beamline, and undulator.

To maximize OTR signal we used a 100-frame sequential acquisition mode, and limited the full beam intensity on the Cu screen to 25-second exposures. We then could integrate the images online with the Hamamatsu HPTA-ver9.1 software or offline with a MATLAB-based program at FNAL. There was an rf macropulse bimodal phase shift that occurred about 10% of the time that also had to be taken into account. A feed-forward phase compensation system was used to flatten the rf waveform that drove the linac and improve electron bunch phase uniformity [1].

CSHR RESULTS

The propagation of the electron beam through the alternating static magnetic fields of an undulator results in the generation of photons. This is initiated through the spontaneous emission radiation (SER) process, but under resonance conditions a favorable instability evolves as the electron beam co-propagates with the photon fields and the electron beam is microbunched at the resonant wavelength in the free-electron laser (FEL). For a planar undulator, the radiation generation process on axis is governed by the resonance condition:

$$\lambda = \lambda_u (1 + K^2/2)/2n\gamma^2, \quad (1)$$

where λ is the UR wavelength, λ_u is the undulator period, K is the undulator field strength parameter, n is the harmonic number, and γ is the relativistic Lorentz factor. In addition, the photon fields of the FEL microbunch the electron beam not only at the fundamental as it co-propagates, but also at the harmonics of that wavelength. We used the 7th harmonic of CSHR at 652 nm to track this process for the first time with a streak camera. It is noted that the CSHR is only emitted from the microbunched portion of the electron beam.

Some of the initial CSHR dual-sweep streak data are shown in Fig. 2. This is a single video image due to the enhanced intensity of the source. The vertical axis spans 300 ps and provides about 2.4-ps FWHM resolution. The horizontal axis sweep range was chosen at 1 μs in this case, and external trigger delays of 0.0, 0.8, and 1.34 μs then were used to step one through the CSHR macropulse. We see two image stripes because the 119.0 MHz sine wave displays the S-band micropulses arriving on both sides of the sine sweep so one phase slew then has the opposite slope.

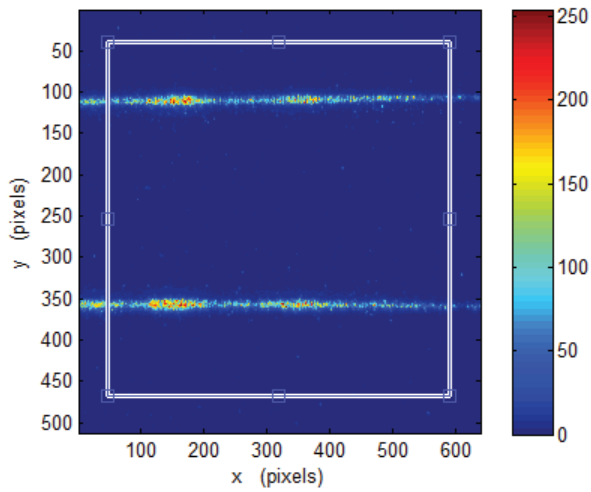

Figure 2: Example dual-sweep streak image of CSHR under lasing conditions using the fastest synchroscan range (R1) vertically (0.62 ps/pixel) and a 1-μs horizontal sweep range. A delay of 0.8 μs positioned this sample in the middle of the CSHR macropulse time.

By setting a 50-pixel wide vertical region of interest (ROI), the amplitude, phase, and bunch length were evaluated in 80-ns widths across the macropulse. The amplitude modulations, including two peaks 320 ns apart, are clearly shown in Fig. 3a as well as a 2-ps phase slew downward to the right in the plot. In Fig. 3b we show the results of Gaussian fits to the time profile of the upper image in each sample. This envelope also shows a correlated reduction in the bunch length with CSHR intensity. The bunch lengths deduced are from 2 to 4 ps (FWHM) after subtracting the camera resolution term [3] in quadrature while assuming a Gaussian temporal profile.

ISBN 978-3-95450-126-7

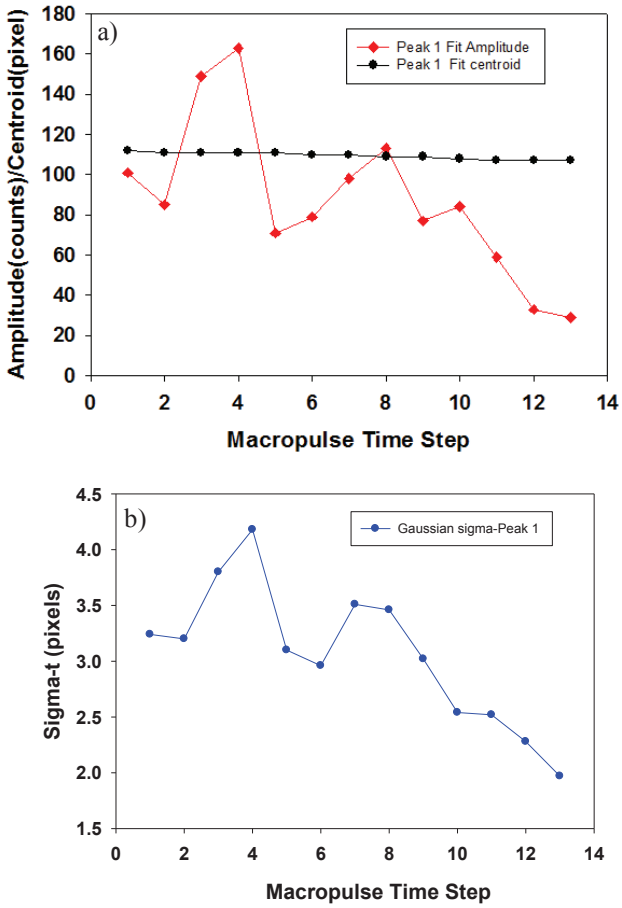

Figure 3: Plots of the variation during the macropulse of a) amplitude and phase and b) bunch length from the image in Fig.2. The vertical calibration is 0.62 ps/pixel.

This variation may be attributed to a CSHR physics effect and/or possibly a space-charge effect within the streak tube at the higher intensities. Further analysis and modeling are warranted.

OTR RESULTS

The OTR data were taken from a Cu screen just after the linac within the diagnostics chicane area. We used a 550-nm longpass filter to limit the chromatic temporal effects to about 2.5 ps FWHM [3]. This term is in addition to the contributions to the total observed image bunch length of actual bunch length, tube resolution, and jitter in the e-beam rf and the synchroscan unit. An example image summed over 100 images is shown in Fig. 4. Again two stripes are seen because the micropulses are at S-band and some arrive on both slopes of the sinusoidal vertical deflection. The delay time is at 0.0 us, and we see OTR earlier than the onset of strong CSHR in the corresponding image. The profile from the ROI shown indicates an average bunch length of ~4 ps FWHM. The low intensity shoulders under and above the two bands, respectively, are attributed to a bimodal phase oscillation in the rf power source during the 100-image acqusition. Such data were also evaluated for phase slew during the macropulse, and they are presented in the next section.

Additionally, sets of 100 images were processed to remove the phase jitter effect by assessing and correcting the shifts in the image position vertically. This was done for a DG535 trigger delay of 1.34 µs and with two different alpha magnet current settings in the microwave gun. The beam bunch lengths determined at the end of the pulse train were 3.5 ps and 4.8 ps (FWHM) for currents of 12.5 and 12.2 A, respectively. Additionally, the phase slews in the last 700 ns of the macropulse were 2 and 2.5 ps for these same settings. The FEL spectral performance was better with the 12.5-A setting.

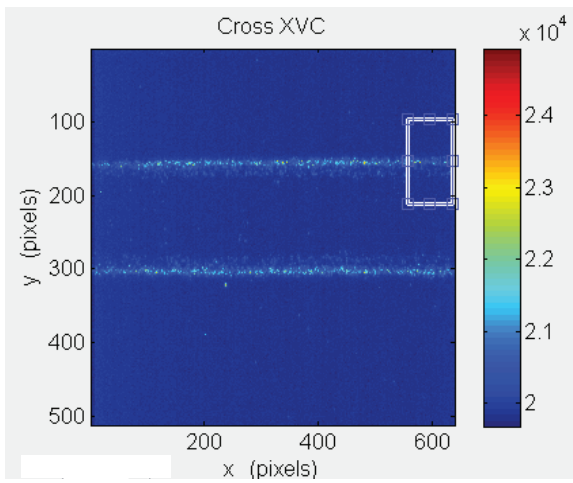

Figure 4: Example 100-image sum of OTR dual sweep images using the fastest synchroscan range (R1) vertically (0.62 ps/pixel) and a 1-µs horizontal sweep range. The external delay was 0.0 µs.

ISBN 978-3-95450-126-7

PHASE ASPECT

By changing the DG535 delay unit setting for the horizontal sweep trigger, we stepped the sampling across the macropulse that was accessible. Unfortunately, the internal delay of the streak unit of about 1 μs prevented one from seeing the early time interval of OTR, although we did detect the onset of the CSHR production. Initial checks of the end point phases of the images for delays of 0.0, 0.8 and 1.34 μs gave us the trends across the macropulse. These are plotted in Fig. 5. Both the OTR and the CSHR sources indicate phase slews of about 7 ps during the total sampled time of about 2.4 μs.

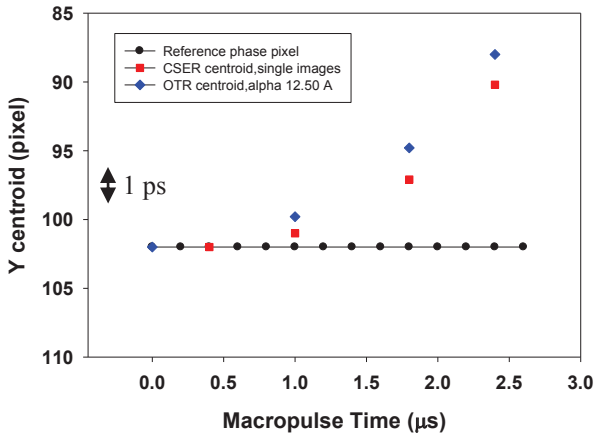

Figure 5: Comparison of the phase slew during the macropulse measured with the streak camera using both the OTR source (blue) and the CSHR source (red).

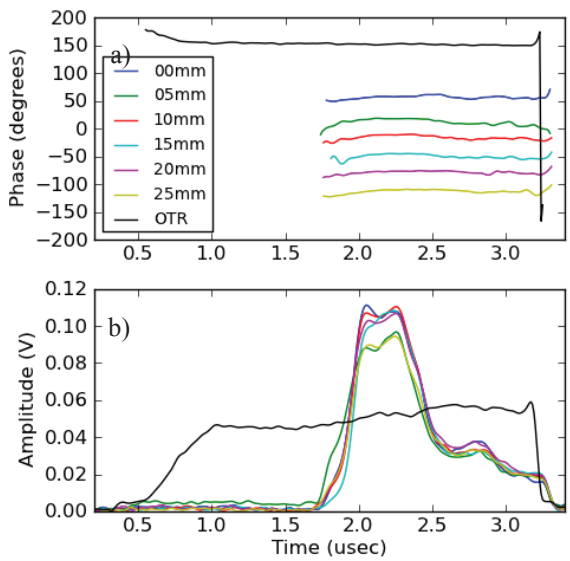

Figure 6: Plots of the variation of OTR and CSHR during the macropulse a) phase and b) signal amplitude using a fast photodiode and mixing with an rf signal.

As an independent check on another run day, the OTR and CSHR signal from a fast photodiode were each mixed with the S-band frequency to obtain phase information as shown in Fig. 6a. The OTR (black) curve indicates a strong slew in the first microsecond of coverage when the FEL does not start up. The CSHR is seen clearly to start later in time after FEL saturation. We also note that the lower plot compares the OTR and CSHR amplitudes for the different optical delay line settings. The strong double peak barely resolved at the 2.0- to 2.3-μs point was more cleanly resolved in the streak data which involve only the 7th harmonic and are sampled spatially by the streak camera entrance slit. Evaluations of this continue.

SUMMARY

In summary, the first streak-camera-based evaluations of the Mark V FEL electron beam have been done. Initial measurements indicate bunch lengths of 3-5 ps FWHM for OTR and some indications of shorter bunch lengths in the CSHR. During the last 2/3 of the macropulse phase slews of about 7 ps were detected, although the FEL itself seemed to accommodate this. The OTR data involved taking sets of 100 images which include rf jitter so dejittering analysis routines are being investigated. Further analysis of CSHR data and modeling of the CSHR effects are planned since the data exhibit interesting temporal effects on both the micro and macro time scales.

ACKNOWLEDGMENTS

The authors acknowledge the loan of the C5680 streak camera system by W. Cieslik of Hamamatsu Photonics and the loan of the compatible 119.0 MHz synchroscan unit by B. Yang of Argonne National Laboratory. The authors also acknowledge the linac operations by the students Foster Ducker, Pardis Niknejadi, and Ian Howe. The first author acknowledges the support of N. Eddy and R. Dixon of FNAL to enable the collaborative tests.

REFERENCES

[1] M. Hadmack et al., Rev. Sci. Instrum. **84,** 063302 (2013).
[2] Douglas J. Bamford and David A.G. Deacon, Nucl. Instrum. and Methods **A296**, 89 (1990).
[3] A.H. Lumpkin, J. Ruan, and R. Thurman-Keup, Nucl. Instrum. and Methods **687**, 92 (2012).

ISBN 978-3-95450-126-7